Polymer 50 (2009) 3617–3625

Contents lists available at ScienceDirect

Polymer

journal homepage: www.elsevier.com/locate/polymer

# Nanostructured polystyrene-*block*-poly(4-vinyl pyridine)(pentadecylphenol) thin films as templates for polypyrrole synthesis

Wendy van Zoelen, Sasa Bondzic, Tatiana Fernández Landaluce, Johan Brondijk, Katja Loos, Arend-Jan Schouten, Petra Rudolf, Gerrit ten Brinke*

*Zernike Institute for Advanced Materials, University of Groningen, Nijenborgh 4, 9747 AG Groningen, The Netherlands*

ARTICLE INFO

*Article history:*
Received 29 April 2009
Received in revised form
2 June 2009
Accepted 8 June 2009
Available online 12 June 2009

*Keywords:*
Block copolymers
Comb-shaped supramolecules
Polypyrrole

ABSTRACT

Polypyrrole has been chemically synthesized on thin film nanostructures obtained from comb-shaped supramolecules of polystyrene-*block*-poly(4-vinyl pyridine) (PS-*b*-P4VP) hydrogen bonded with pentadecylphenol (PDP). PDP was washed from thin films of cylindrical and lamellar self-assembled comb-copolymer systems, which resulted in removal of the upper layers of microdomains, leaving single cylindrical and lamellar layers covering a substrate, with P4VP segregated at the bottom as well as at the free air interface. This P4VP was complexed with $Cu^{2+}$ ions, after which chemical oxidation polymerization of pyrrole resulted in a thin polypyrrole layer covering the nanostructured block copolymer. The use of a catalytic amount of bipyrrole greatly improved the quality of the obtained product. The conductivity was measured to be $\sim 0.7\ S\ cm^{-1}$.

© 2009 Elsevier Ltd. All rights reserved.

## 1. Introduction

Since their discovery, electrically conductive polymers such as polyacetylene, polythiophene, polyphenylene, and polypyrrole have been extensively studied due to their interesting electronic properties and possible applications as battery electrodes, sensors and solid-state devices [1–5]. Especially the fabrication of nanostructured devices has received considerable attention, as these have proven to be even more effective than their larger sized counterparts, for example in sensor applications due to the greater exposed surface area of nanostructured materials [6], or due to their higher conductivity as compared to bulk samples [7]. Thin films of conducting polymers are appealing for optoelectronic device applications, which often require polymeric transparent electrodes for the improvement of device performance and fabrication of polymer only devices [8]. Among the conducting polymers, polypyrrole has always remained an attractive option due to its relatively high environmental stability and electrical conductivity, and easy preparation. On the other hand, a disadvantage of polypyrrole, is that it has poor mechanical properties. It can be prepared either by chemical or by electrochemical oxidation polymerization. The electrochemical method has remained far more popular due to the superior properties of the obtained material as compared to chemically prepared polypyrrole, which is usually obtained as a powdery precipitate. Its properties very much depend on the reaction conditions, such as the nature and concentration of the oxidant, reactant stoichiometry, reaction medium, temperature, and reaction time [9–12]. Nevertheless, an advantage of the chemical method is that it can be used to polymerize polypyrrole onto a polymeric template, for example to obtain material with better mechanical properties or to obtain nanostructured polypyrrole [13,14]. Especially poly(4-vinylpyridine) (P4VP) has been used in this respect, due to the ability of P4VP to form complexes with various oxidants, while these retain their ability to oxidize pyrrole [15–24].

P4VP containing *block copolymers* are interesting candidates as templates, due to the nanoscale ordered structures that can be formed by self-assembly. Especially when ordered in thin films, such nanostructures offer great possibilities for use in nanotechnology applications [25]. In thin films, the tendency of the block with the lower surface free energy to segregate at the air interface, and that of the block with the lowest interfacial energy to segregate at the substrate interface usually cause the formation of terraces of microdomains oriented parallel to the substrate when the initial film thickness is incommensurate with the microdomain period. This implies that in P4VP-based block copolymers, P4VP will generally not segregate at the air interface due to its high surface free energy. However, the use of PS-*b*-P4VP(PDP) comb-shaped supramolecules, where PS denotes polystyrene and PDP denotes pentadecylphenol amphiphiles that hydrogen bond to the pyridine units of P4VP, offers an attractive option to avoid this effect. The ability of these supramolecules to microphase separate into so-called structures-*within*-structures was first recognized by

* Corresponding author.
*E-mail address:* g.ten.brinke@rug.nl (G. ten Brinke).

0032-3861/$ – see front matter © 2009 Elsevier Ltd. All rights reserved.
doi:10.1016/j.polymer.2009.06.012

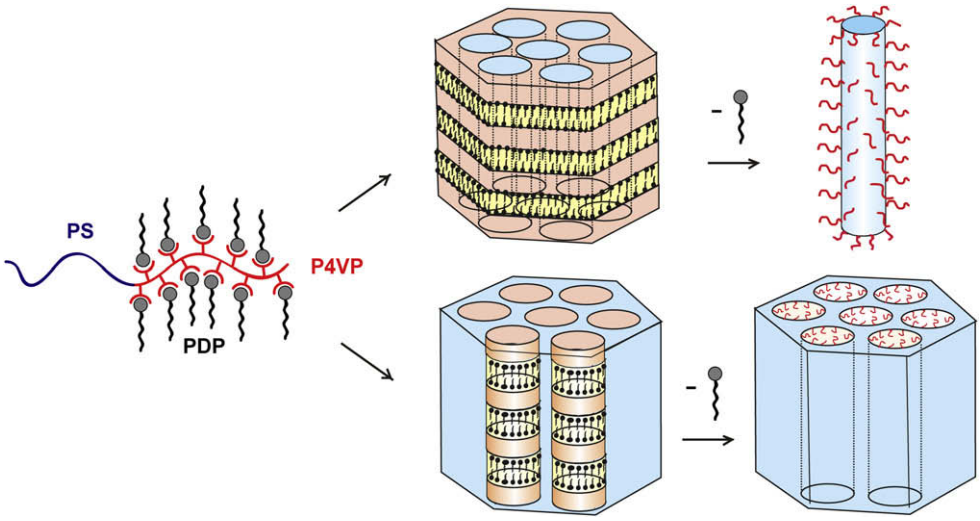


**Fig. 1.** Cylinders-*within*-lamellae and lamellae-*within*-cylinders formation of PS-*b*-P4VP(PDP) comb-shaped supramolecules. By washing away PDP, nanorods and nanoporous structures are easily obtained.

Ruokolainen et al. [26]. The easy removal afterwards of the PDP molecules by simple dissolution is a great advantage for nanomaterial fabrication (Fig. 1) [27].

In thin films of these supramolecules on silicon oxide ($SiO_2$), the entire comb-block generally segregates at the air interface as well as at the substrate interface, due to the preferential interactions of PDP with air and of P4VP with $SiO_2$. Just as in most other simpler diblock copolymer systems, this leads to the formation of terraces of parallelly oriented microdomains. Subsequently washing away PDP easily results in *single*, *uniform* cylindrical or lamellar layers, depending on the self-assembled state, covering the substrate (Fig. 2) [28]. This not only takes away the need to carefully control the film thickness in order to avoid terrace formation when a single microdomain layer is desired, but also results in P4VP being present at the air interface. In the present paper, such nanostructured templates from thin films of PS-*b*-P4VP(PDP) comb-shaped supramolecules, obtained by exfoliating the top layers of microphase separated thin films of asymmetric PS-*b*-P4VP(PDP) with a high P4VP(PDP) weight fraction as previously described in Ref. [28], have been used to create transparent conducting thin films and polypyrrole/PS-*b*-P4VP hybrid nanorods via template synthesis with $CuCl_2$ as an oxidant. The use of a catalytic amount of bipyrrole proved to have a significant influence on the polymerization mechanism and the quality of the obtained product.

## 2. Experimental section

### 2.1. Materials and sample preparation

#### 2.1.1. Chemicals

Two different block copolymers, P3546-S4VP ($M_n$(PS) = 20,000 g mol$^{-1}$, $M_n$(P4VP) = 19,000 g mol$^{-1}$ and $M_w/M_n$ = 1.09) and P110-S4VP ($M_n$(PS) = 47,600 g mol$^{-1}$, $M_n$(P4VP) = 20,900 g mol$^{-1}$ and $M_w/M_n$ = 1.14) were obtained from Polymer Source, Inc. and used as-received. Pentadecylphenol (PDP) was purchased from Aldrich and was recrystallized twice from petroleum ether (40–60 w/w) and dried in a vacuum at 40 °C. Pyrrole (99% pure, Acros) was distilled from calcium hydride and stored at −15 °C until use. Analytical grade solvents were all used as-received. 2,2′-Bipyrrole was synthesized according to an established procedure [29,30].

#### 2.1.2. Substrate preparation

Double side polished silicon (Si) substrates of ~1 cm$^2$ with a native silicon oxide layer on the surface were cleaned by immersion in a 70/30 v/v piranha solution of concentrated $H_2SO_4$ and $H_2O_2$ (30%) at 60 °C for 1 h, thoroughly rinsed with Milli-Q water, treated ultrasonically in methanol for 15 min, and dried under a stream of nitrogen.

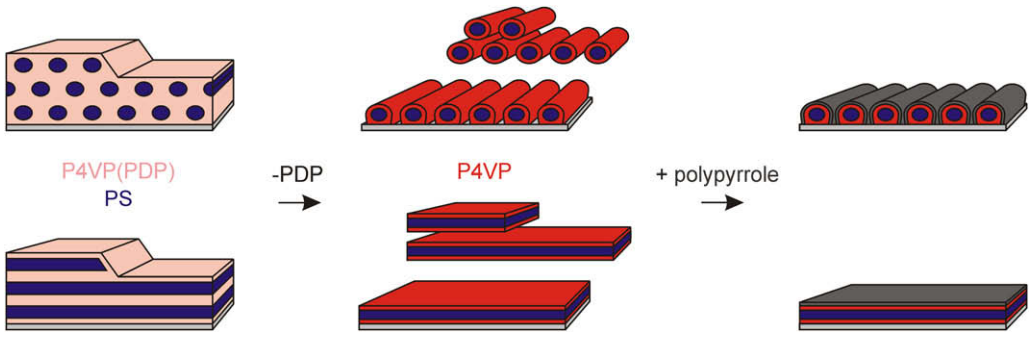


**Fig. 2.** Schematic representation of polypyrrole formation on lamellar and cylindrical templates created from PS-*b*-P4VP(PDP) supramolecules. Preferential interactions of the P4VP(PDP) comb with both interfaces leads to a parallel orientation of microdomains. By subsequent washing in ethanol, the top layers of cylinders/lamellae are exfoliated and a uniform monolayer of cylinders/lamellae remains at the substrate. P4VP is segregated at both interfaces. After complexation of P4VP with $Cu^{2+}$ ions, pyrrole is polymerized onto the polymeric template.

*2.1.3. Thin film preparation*

PS-*b*-P4VP and PDP were dissolved in $CHCl_3$ and stirred for at least 2 h to yield ~1 wt% stock solutions. These solutions were diluted and spin coated at speeds between 2000 and 5000 rpm to yield films of ~70 nm thickness. Subsequently, the films were annealed in chloroform vapor in a small sealed chamber for ~20 h. The temperature of the polymer samples $T_p$ was kept at 24 °C with a Tamson heating circulator, while the temperature of the included solvent reservoir $T_s$ was kept at 20 °C with a Lauda RC6 CP refrigerated circulator. After annealing the lid was lifted from the setup and solvent evaporated within a fraction of a second. PDP was washed from the films by ultrasound treatment in ethanol for at least 5 min, only leaving one polymer layer at the $SiO_2$ interface.

*2.1.4. Copper complexation*

The thin films were soaked for various amounts of time in a filtered 0.25 M solution of hydrous $CuCl_2$ in methanol, after which the samples were thoroughly rinsed and washed for 1 min in methanol under ultrasound to remove uncomplexed copper.

*2.1.5. Pyrrole polymerization*

The $Cu^{2+}$ complexed samples were soaked for various amounts of time in methanol solutions of pyrrole (various concentrations, both with and without 2,2′-bipyrrole), after which the samples were ultrasonically treated for 1 min in methanol.

*2.2. Instrumental methods*

*2.2.1. Atomic force microscopy*

Tapping mode AFM was performed on a Digital Instruments Enviroscope AFM equipped with a Nanoscope IIIa controller using Veeco RTESPW silicon cantilevers ($f_0 = 240$–$296$ kHz and $k = 20$–$80$ N/m as specified by the manufacturer). Film heights were measured by scratching the polymer layer from the silicon oxide surface with a razorblade, being careful not to damage the substrate itself, after which scans with a 1:8 ratio were taken at the edge between the polymer layer and the silicon substrate to minimize distortion along the slow scanning axis. The height of the films was measured within a 1.5% error margin by fitting a plane to the bare substrate and plotting a depth profile using Digital Instruments Nanoscope software.

*2.2.2. Fourier transform infrared spectroscopy*

Transmission FTIR measurements were performed on a Bruker IFS 66v/S spectrometer equipped with a DTGS detector. All spectra were measured at a resolution of 4 $cm^{-1}$ and are averages of 2400 scans. The spectrum of a clean silicon wafer was used as a reference.

*2.2.3. X-ray photoelectron spectroscopy*

The samples were introduced through a load look system into an SSX-100 (Surface Science Instruments) photoemission spectrometer with a monochromatic Al Kα X-ray source ($h\nu = 1486.6$ eV). The base pressure in the spectrometer during the measurements was $10^{-10}$ mbar. The photoelectron takeoff angle was 37°. The energy resolution was set to 1.3 eV to minimize measuring time. Sample charging was compensated for by directing an electron flood gun onto the sample. XPS binding energies were referenced to the carbon signal at 284.5 eV. Spectral analysis included a Shirley background subtraction and a peak deconvolution that employed Gaussian and Lorentzian functions in a least-square curve-fitting program (WinSpec) developed at the LISE, University of Namur, Belgium.

*2.2.4. Conductivity measurements*

Conductivity measurements were performed in vacuum on polypyrrole coated single lamellar PS-*b*-P4VP layers that were prepared on silicon substrates with a ~300 nm thick insulating $SiO_2$ layer. Two ~60 nm thick gold electrodes with a width of 4 mm and 60 μm separation were evaporated onto the polypyrrole, after which I-V curves were recorded using a Keithley 4200 SCS.

## 3. Results and discussion

*3.1. Template formation*

In Ref. [28], it was shown how a uniform monolayer of parallel cylinders could be obtained by annealing the cylindrical PS-*b*-P4VP(PDP) comb copolymer system P110$(PDP)_{1.5}$ (the subscript implies the presence of 1.5 PDP molecule per pyridine unit), with a film thickness of two layers of parallel cylinders or more, in chloroform vapor and subsequently washing away PDP and the top layers of cylinders with ethanol. Less attention was focused on the P3546$(PDP)_{0.1}$ system containing only a small amount of PDP,

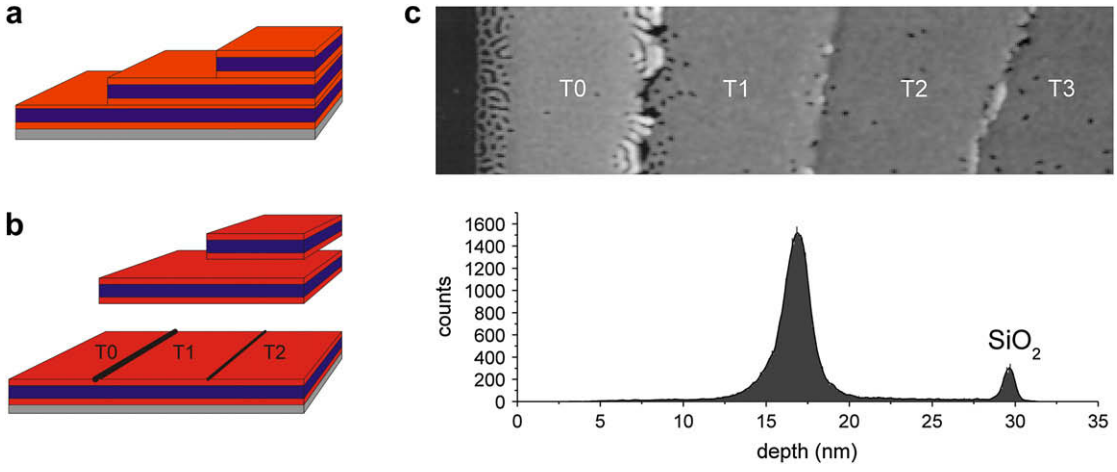


**Fig. 3.** (a) Terrace structure of a lamellar thin PS-*b*-P4VP(PDP) film. (b) Thin film structure after washing away PDP and removing the top layers of lamellae. The former terrace edges can still be observed in the bottom layer (black lines). (c) AFM height image and depth profile of a P3546$(PDP)_{0.1}$ thin film after chloroform vapor annealing and ultrasound treatment in ethanol (image size = 3 × 0.75 μm). A plane has been fitted to the scratch on the left, after which a depth profile was created. The presence of a single peak indicates that the bottom layers of all terraces, including the first one, have the same height, however, the defect density in the bottom layer at the transition from the former lowest (T0) to the former second terrace (T1) is relatively high. This was also the case for cylindrical samples, which is why the minimum film thickness before PDP removal was chosen to be 2 microdomain spacings.

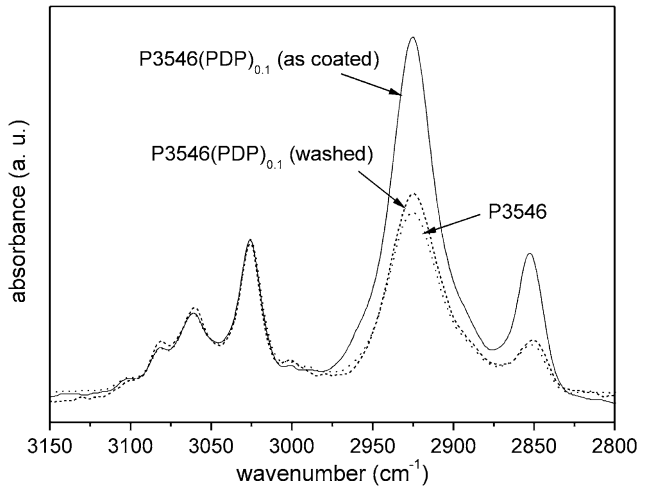


**Fig. 4.** Transmission FTIR spectra of a P3546(PDP)$_{0.1}$ thin film before and after ultrasound treatment in ethanol compared with the FTIR spectrum of the pure diblock copolymer.

which forms a single lamellar layer with uniform thickness after ultrasound treatment of an annealed film (Fig. 3).

Unlike for the cylindrical sample [28], the transition between the terraces is never smooth, and thus a truly uniform monolayer can not be obtained; when the samples are washed in ethanol, P4VP chains are present on the entire surface, also at defect locations, which after templated polymerization of polypyrrole will result in a continuous layer of polypyrrole covering the entire sample, with only some height defects near a former terrace edge.

Both the lamellar as well as the cylindrical layers have been used as templates for polypyrrole polymerization. In Fig. 4, typical FTIR spectra of a lamellar thin film before and after ultrasound treatment in ethanol are shown, together with the spectrum of a pure block copolymer thin film. The decrease in intensity of the $CH_2$ bands at 2920 and 2850 $cm^{-1}$ relative to the aromatic CH bands between 3100 and 3000 $cm^{-1}$ indicates that the main part of PDP is washed from the system in the process of exfoliating the top lamellar layers from the substrate, although it can not be excluded that a small amount of PDP remains in the sample.

### 3.2. Templated pyrrole polymerization

The conductive properties of conjugated polymers such as polypyrrole depend on several factors. First of all, all conducting polymers are semiconductors, which have to be doped to produce mobile charge carriers. Therefore, the level of doping as well as the used dopant ion largely influence the conductivity of the polymer chains. Furthermore, the conductivity also depends on the charge transport between polymer chains. Charge carriers can more easily be transferred between polymer chains in highly ordered samples, and also within the polymer chain, a higher degree of order results in better transport properties. Finally, the conjugation length of the polymer chain plays an important role. The longer the chain of alternating single and double bonds, the better is the conductivity.

*Electrochemical* polymerization of pyrrole proceeds only when the potential is sufficiently high to oxidize the monomer, whereas too high potentials and high pH values easily lead to excess oxygen uptake in the polymer chain [31]. This 'overoxidation' may be caused by nucleophilic attack of $OH^-$ ions originating from dissociation of water in, or as, the solvent [32,33], which introduces covalently bound OH and C═O groups to the polymer, disrupting the conjugation length and deteriorating its conductive properties. However, the oxidation potential is easily controllable, and therefore the quality of the obtained material can be optimized. In *chemically* synthesized polypyrrole, factors such as solvent, reaction temperature, time, nature, and concentration of the oxidizing agent all affect the oxidation potential of the solution as well as the doping level of the polymer, which highly complicates the search for optimal reaction conditions [34].

Nevertheless, for chemical oxidative polymerization, $FeCl_3$ has widely been accepted as the oxidant yielding polypyrrole with the best properties. However, it has a big disadvantage in terms of P4VP templated polymerization, as complexed Fe ions can no longer polymerize pyrrole monomers [24]. That is why in this study, the also frequently utilized oxidizing agent $CuCl_2$ has been used. If P4VP is present in excess, $Cu^{2+}$ ions can form a complex with a maximum of four pyridine units, which do not necessarily have to originate from the same polymer chain, resulting in crosslinking [35]. When $Cu^{2+}$ ions are present in excess, on average 2 VP units are complexed to the copper ion [36]. Nonetheless, irrespective of the number of attached ligands, all copper ions can induce pyrrole polymerization (Fig. 5) [24].

Fig. 6 shows the FTIR results of complexation of P4VP in a solution of 0.25 M $CuCl_2$ in methanol. Already after 15 min of immersion in the $CuCl_2$ solution, complexation of $Cu^{2+}$ with the pyridine rings has taken place, as evidenced by the IR shifts of the CN stretching bands of the pyridine ring at 1600 and 1415 $cm^{-1}$ to 1625 and 1425 $cm^{-1}$, respectively [37]. An extra feature in the form of a band at ~1640 $cm^{-1}$ can also be observed, which indicates the formation of pyridine *N*-oxides or quaternized pyridine. Its presence in a nanorod-like thin film that was created without PDP (see Fig. 7 for more details) indicates that the cause can not be found in a reaction with any remaining PDP.

The relative invisibility of the ~1640 $cm^{-1}$ band in thicker films of block copolymers complexed with $Cu^{2+}$ on the other hand [38] hints that it is caused by a surface effect. In silica gels doped with $[Cu(C_5H_5N)_4]^{2+}$ complexes ($C_5H_5N$ = pyridine), the slightly acidic residual surface SiOH groups have been found to protonate pyridine units, after which a chemical bond was formed between the complexed copper and the hydroxyl oxygens on the surface of the silicon [39].

$$Si{-}OH + C_5H_5N \rightarrow Si{-}O^- + C_5H_5NH^+ \quad (1)$$

$$Si{-}O^- + H_2O + [Cu(Py)_4]^{2+} \rightarrow [Si{-}O{-}Cu(Py)_4(H_2O)]^+ \quad (2)$$

A comparable mechanism may also apply in our case, which would explain why XPS spectra of all complexed samples indicate the presence of two copper species (Fig. 8). Two peaks were identified in the Cu2p spectra: $Cu^+$ at 935 eV and $Cu^{2+}$ at 942.7 eV [40].

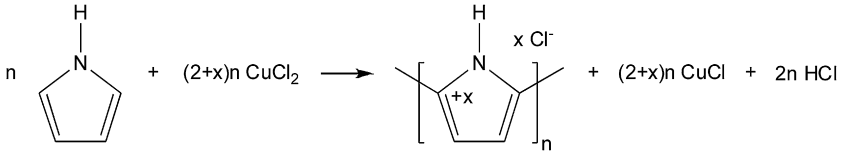


**Fig. 5.** Schematic representation of chemical pyrrole polymerization using $CuCl_2$ as an oxidant. The reaction results in the doped form of the polymer.

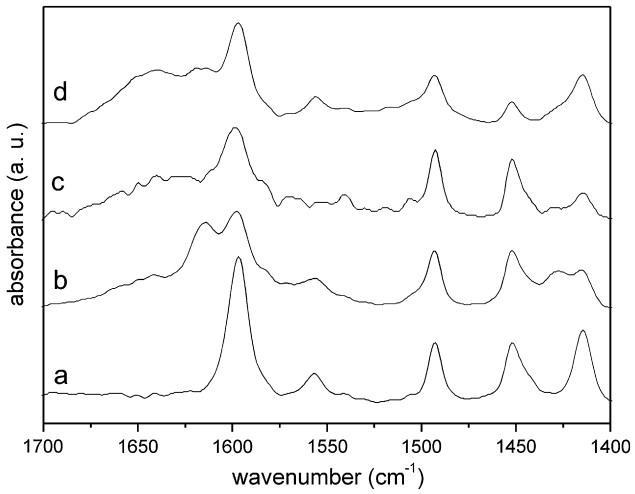


**Fig. 6.** Transmission FTIR spectra of (a) a lamellar P3546(PDP)$_{0.1}$ thin film after ultrasound treatment in ethanol and (b) subsequent complexation in a 0.25 M $CuCl_2$ solution. (c) As part b, but for cylindrical P110(PDP)$_{1.5}$. (d) As part b, but for semi-cylindrical P3918, created without PDP (see Fig. 7). The total absorbance in parts c and d was approximately 40% lower due to the smaller amount of cylindrical material as compared to a lamellar layer, which also contributes to the relative high amount of noise in part c.

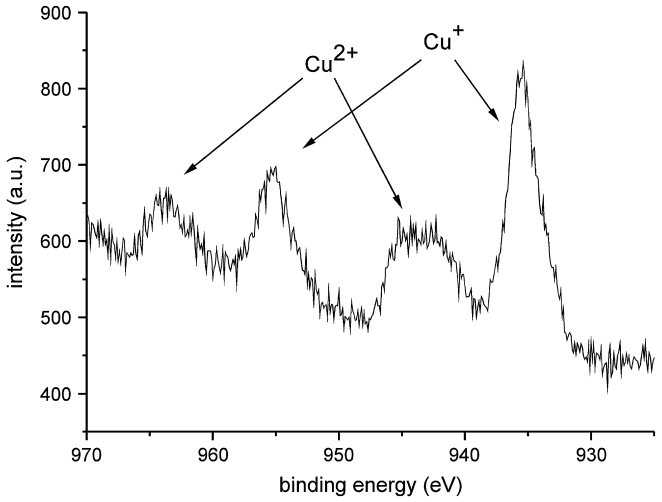


**Fig. 8.** X-ray photoelectron spectrum of the Cu2p core level region of a P110 nanorod film after 1 h of complexation in a 0.25 M $CuCl_2$ solution.

The three nitrogen species found by IR are also confirmed by XPS. In Fig. 9, the XPS signal of the nitrogen 1s core level of a P110 nanorod film after copper complexation is shown together with the least square best fits. In this N1s spectrum three peaks were observed, one with the N1s component at a binding energy of 399.2 eV, assigned to free pyridine, and a second component at 400 eV assigned to complexed pyridine. A third peak component at 400.7 eV corresponds to quaternized pyridine; all peaks are in agreement with literature [41].

Furthermore, the extra IR band at 1640 $cm^{-1}$ is larger in nanorod samples than it is in the lamellar one. As the silicon interface in the lamellar layers is shielded by a layer of PS, it is more difficult for the copper ions to reach the P4VP at the silicon interface, while in the nanorod samples, this interface is largely uncovered. Longer complexation times than the normally applied 15 min or the use of higher $CuCl_2$ concentrations had little effect on the IR spectra, indicating that complexation was complete.

The polypyrrole quality has often been related to the concentration of the oxidizing agent and the monomer:oxidant ratio. In the case of templated polymerization, the concentration of the oxidant is a complicated matter, first of all because the ions are connected to the P4VP surface, and secondly because the degree of complexation is not known. The thickness of a lamellar film increased ~13% after copper complexation. Assuming the maximum complexation of two pyridine units per copper ion and a $CuCl_2$ density of 3.38 g $cm^{-3}$, the thickness increase of a lamellar film can only be ~10% at maximum. However, the density of complexed copper is most likely much less than the 3.38 g $cm^{-3}$ for the crystalline material, and pyridine units near the silicon interface are likely less complexed than pyridine units at the air interface, making the degree of complexation hard to estimate.

Nevertheless, although the degree of complexation and hence the oxidant concentration was unknown, it could be kept constant by complexing all used samples longer than 15 min in a 0.25 M $CuCl_2$ solution (typically 1 h), the time after which constant IR spectra indicated complexation to be complete. Thus, the only concentration that can be varied is the pyrrole concentration. Furthermore, protic solvents and especially methanol have proven

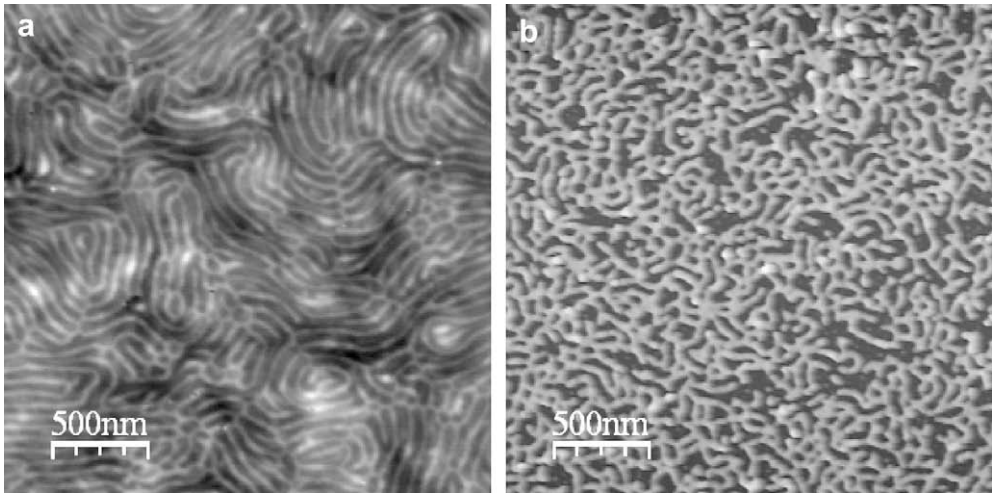


**Fig. 7.** AFM height images of a ~70 nm P3918 ($M_n$(PS) = 20,500 g $mol^{-1}$, $M_n$(P4VP) = 36,000 g $mol^{-1}$ and $M_w/M_n$ = 1.08) thin film after (a) annealing in saturated vapors of a 50/50 mixture of chloroform and ethanol ($\Delta z$ = 21 nm), and (b) subsequent ultrasound treatment in ethanol ($\Delta z$ = 55 nm). The obtained "nanorods" are not well ordered, but no PDP was used in the process.

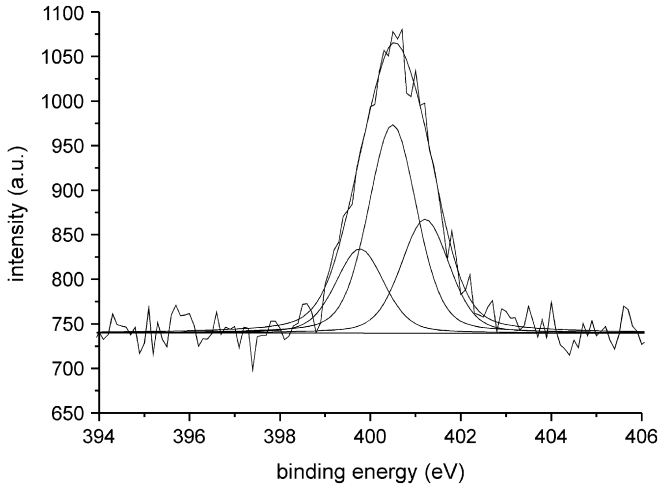


**Fig. 9.** X-ray photoelectron spectrum of the N1s core level region of a P110 nanorod film after 1 h of complexation in a 0.25 M $CuCl_2$ solution.

to yield the best quality products [12], and by using solvent mixtures of methanol and acetonitrile or adding $FeCl_2$ even more suitable oxidation potentials could be realized [10,12]. However, these studies were performed on systems where $FeCl_3$ was used as an oxidizing agent, and solvents may have a different influence on the oxidation potential of $CuCl_2$ solutions. Nevertheless, in this study methanol was chosen as a common solvent for all experiments, not in the last place because it is a good solvent for P4VP.

Complexed lamellar films were treated by immersion in solutions of pyrrole in methanol for 16 h. Treatment in a 1 M pyrrole solution did not result in any visible effect in IR results, indicating that no reaction has taken place due to a too low reactant concentration. Treatment in 5 M pyrrole on the other hand, resulted in the FTIR spectrum shown in Fig. 10.

The shoulder at 1640 $cm^{-1}$ caused by the quaternized pyridine does not seem to be effected, yet both peaks of complexed nitrogen atoms at 1615 $cm^{-1}$ and 1430 $cm^{-1}$ have largely disappeared, indicating that the complexed $Cu^{2+}$ species have been reduced to free $Cu^{+}$. Nevertheless, a clear indication of polypyrrole formation in the form of characteristic polypyrrole peaks can not be observed. The only extra band that is clearly present is a small carboxyl band at 1710 $cm^{-1}$. As mentioned before, this band has been observed in many pyrrole samples, chemically as well as electrochemically prepared, and is an indication of pyrrole overoxidation. C=O bonds are formed, which break the conjugation in polypyrrole, and lead to poorly conducting products. In reactions with $FeCl_3$ as an oxidant, Thiéblemont et al. [33] concluded that short polymer chains which are formed in the beginning of the synthesis are more susceptible toward overoxidation. Furthermore, they found that the polypyrrole formation rate is proportional to the square of the oxidant concentration, while its overoxidation rate appears to be only proportional to this concentration. In accordance, higher oxidant concentrations give better products. In the case of the thin films used here, the oxidant concentration is probably so low, that only very short polymer chains are produced, which are all overoxidized, presumably even to short, soluble molecules such as maleimide that are not present in the film anymore after washing in ultrasound. However, as the oxidant concentration in the thin films cannot be increased, another method to produce polypyrrole was sought.

### 3.3. Influence of bipyrrole

In a recent study Tran et al. confirmed that dimer formation is the rate determining step in polypyrrole synthesis [42]. Bipyrrole has a lower oxidation potential than pyrrole and can serve as a nucleation center for growing polymer chains. Therefore, the intentional introduction of bipyrrole into the reaction mixture greatly enhances the rate of polymerization. This also implies that there are not many short chains present in the reaction mixture, which should substantially decrease the extent of overoxidation. That this is indeed the case can be seen in Fig. 11.

Reaction in a mixture of 1 M pyrrole and 0.01 M of bipyrrole clearly results in polypyrrole, as can be concluded from the present characteristic polypyrrole bands at 1560 $cm^{-1}$ (C=C stretching vibration) [43] and 1370 $cm^{-1}$ (N–C stretching) [43] not present before polymerization, and the increase in film thickness of a 15.4 nm thick lamellar film before polymerization to 28.0 nm afterward. The featureless decrease in absorption, visible from 4000 to 1700 $cm^{-1}$ has been assigned to the tail of the electronic absorption band located in the near infrared region [43]. The bands at 3110 and 3435 $cm^{-1}$ are due to C–H and N–H stretching vibrations, respectively [44]. However, the obtained polypyrrole still clearly contains carbonyl defects as evidenced by the band at

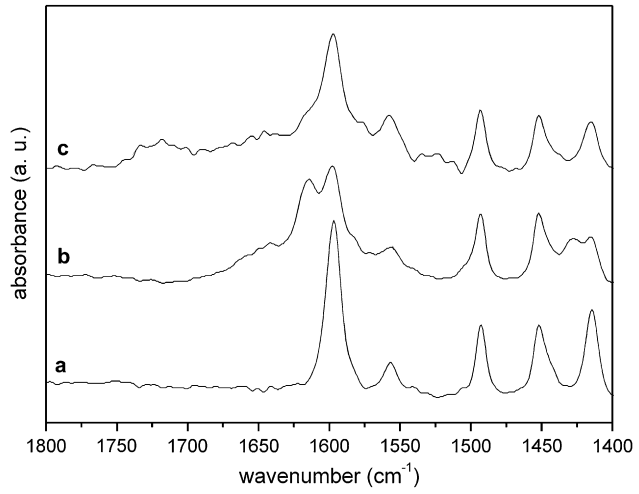


**Fig. 10.** Transmission FTIR spectra of (a) a lamellar P3546$(PDP)_{0.1}$ thin film after ultrasound treatment in ethanol and (b) subsequent complexation in a 0.25 M $CuCl_2$ solution. (c) FTIR spectrum of a $Cu^{2+}$ complexed lamellar layer after 16 h in a 5 M pyrrole solution.

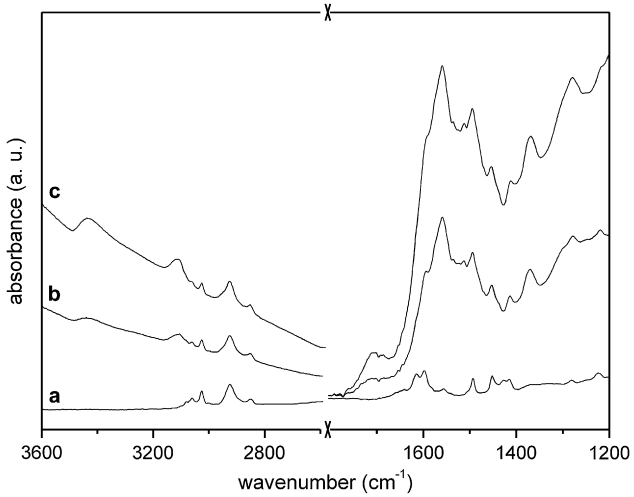


**Fig. 11.** FTIR spectra of (a) $Cu^{2+}$ complexed P3546 lamellar layer, (b) $Cu^{2+}$ complexed P3546 after 16 h in a solution of 1 M pyrrole and 0.01 M bipyrrole, and (c) $Cu^{2+}$ complexed P3546 after 16 h in a solution of 5 M pyrrole and 0.01 M bipyrrole.

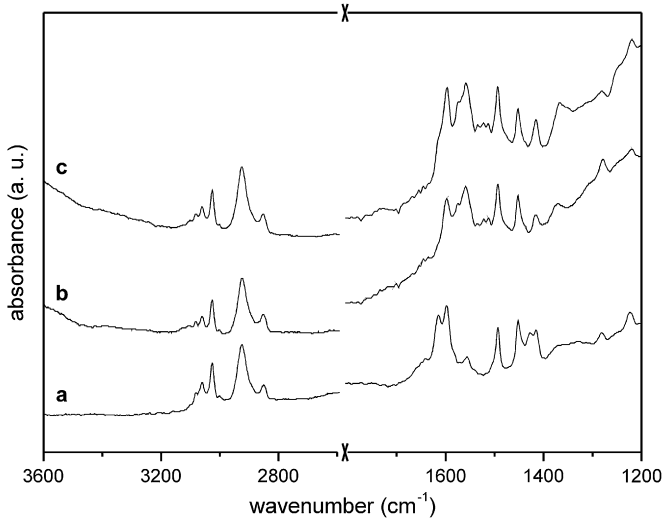


**Fig. 12.** FTIR spectra of (a) a P3546 lamellar layer complexed with $Cu^{2+}$, (b) $Cu^{2+}$ complexed P110 cylinders after 16 h in a 1 M pyrrole and 0.01 M bipyrrole solution, (c) $Cu^{2+}$ complexed P3546 lamellae after 1 h in a 1 M pyrrole and 0.01 M bipyrrole solution.

1710 $cm^{-1}$. Reaction in 5 M pyrrole together with 0.01 M of bipyrrole logically resulted in higher polypyrrole yields (41.5 nm and higher intensity of IR peaks), yet the relative amount of carbonyl defects remained comparable. In both cases, adjustment of the bipyrrole concentration to twice the value also did not result in a noteworthy difference.

Assuming a maximum complexation of 2 pyridine units per $Cu^{2+}$ ion, and keeping in mind that every pyrrole unit has to be oxidized by 2 $Cu^{2+}$ ions to be incorporated in the polymer chain, the maximum thickness increase can only be ~10%. In both cases, the thickness increase was considerably higher, even over 100% for the 5 M pyrrole + 0.01 M bipyrrole solution. This indicates that the $Cu^{+}$ ions that are a product of the monomer activation are reoxidized to active $Cu^{2+}$ ions by oxygen [45]. In this way, $Cu^{2+}$ ions may oxidize multiple pyrrole units, explaining the high yields. This assumption is furthermore supported by the fact that the solutions which held the silicon wafers turned black much faster than an unused solution, indicating polypyrrole formation within the solution. This non-templated polypyrrole formation is only possible if the complexed $Cu^{2+}$ species that were transformed to freely dissolved $Cu^{+}$ were reoxidized again.

Finally, the reaction time is an important factor on which the quality of the obtained polymer depends. Longer reaction times obviously result in higher yields, yet the conductive quality of the obtained polymer is usually optimal at lower yields [12]. The optimal polymerization time depends on the other reaction conditions such as temperature and reactant concentration, the latter one because it influences the oxidation potential [12]. Fig. 12 shows the FTIR spectrum of a $Cu^{2+}$ complexed lamellar film that was reacted in a 1 M pyrrole and 0.01 M bipyrrole solution for only 1 h.

The polypyrrole yield is very low, as can be concluded from the lower peak intensities as compared to Fig. 11, as well as the low thickness increase (15.4–19.7 nm, ~25%), on the other hand, the IR band at 1710 $cm^{-1}$ is absent, indicating that substantially less overoxidation has taken place. This means that for the studied reactions with bipyrrole, the overoxidation mainly occurs in a later stage of the reaction. In an early stage, most bipyrrole units will quickly react to form long polymer chains. In a later stage, the $Cu^{2+}$ concentration will be substantially lower, and it will take longer for a starting polymer chain to be oxidized by $Cu^{2+}$ and grow. This means that there are relatively more short chains present, and these chains are susceptible towards overoxidation. Furthermore, the rms roughness of the longer reacted samples ($1.9 \pm 0.2$ nm for the 1 M pyrrole + 0.01 M bipyrrole solution) is substantially higher than the roughness of the sample that was reacted for only 1 h in the same solution. With 0.7 nm, this roughness is the same as that of the pure block copolymer film. In the samples that were reacted for 16 h, individual polypyrrole particles appear to be present (Fig. 13).

This is consistent with the conventional synthesis mechanism of polypyrrole, which proceeds slowly. Embryonic nuclei have the opportunity to diffuse to heterogeneous nucleation sites, which leads to agglomerated structures of different starting chains growing together, whereas in early stage reactions with bipyrrole, homogeneous nucleation dominates, which means that polymer chains grow from the site where they were started, which in bulk solutions leads to nanofibers [42], and in our templated case presumably to smoother surfaces.

For the nanorod samples, the results slightly differ. In this case, even after 16 h of reaction, no carbonyl band is observed in FTIR. Furthermore, even after the long reaction time, the polypyrrole yield is very low, as can be concluded from the low intensity of the IR bands. This low yield may be explained by the relatively low amount of $Cu^{2+}$ species in the sample as compared to the lamellar samples. The absence of the carbonyl band after this long reaction time is more difficult to explain, although it can only have a positive effect on the conductive properties of the obtained polypyrrole. These

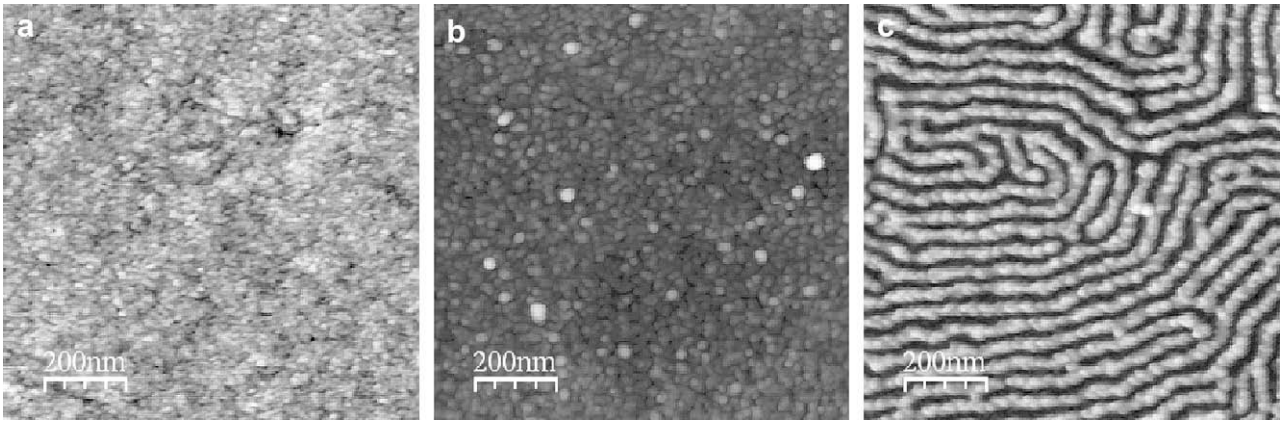


**Fig. 13.** Height AFM images of (a) polypyrrole on lamellar P3546 after 1 h in 1 M pyrrole and 0.01 M bipyrrole ($\Delta z = 6$ nm), (b) as part a, but after 16 h ($\Delta z = 28$ nm), (c) as part b, but for cylindrical P110 ($\Delta z = 32$ nm), the AFM image is comparable to that of a 1 h reacted P110 sample.

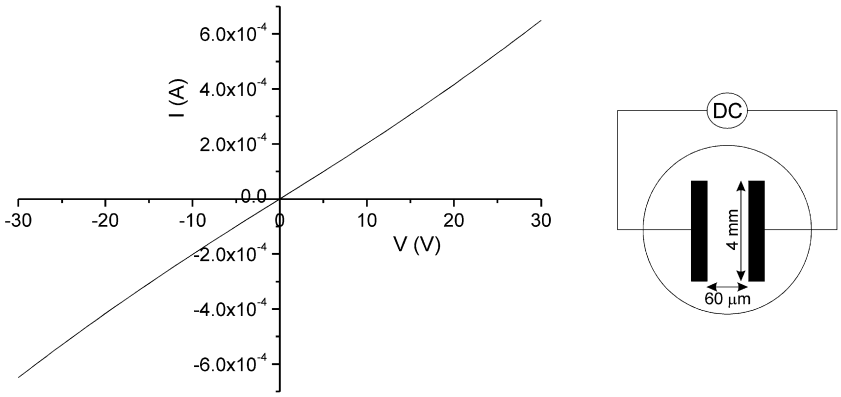


**Fig. 14.** *I–V* plot of a ~4 nm polypyrrole layer on a ~15 nm lamellar P3546 film and schematic drawing of the used setup.

properties could be tested by performing conductivity measurements, however, reliable conductivity measurements on nanorod samples are hard to conduct. For normal 4-point or 2-point probe measurements for example, a connecting path should be created between the probes. This is difficult to obtain for the non-macroscopically aligned nanorod samples, and the measured conductivity will be very much subject to the number of connecting paths, which can be variable for every nanorod sample as it depends on the ordering of the rods and the exact amount of defects. Furthermore, because of the low thickness of the polypyrrole film covering the samples, the current trough the film will be very low, meaning that very sensitive equipment should be employed.

### 3.4. Conductivity measurements

For conductivity measurements on the lamellar samples, only the last problem has to be dealt with, and this problem is not insurmountable. By placing two line electrodes only several microns apart, a large enough current to measure the conductivity should be able to flow. This was realized by evaporating two ~60 nm thick gold electrodes with a width of 4 mm and 60 μm separation onto a polypyrrole sample that was reacted for 1 h in a 1 M pyrrole with 0.01 M bipyrrole solution. The ramping voltage was varied from −30 V to 30 V, and resulted in a straight *I–V* curve, indicating an average conductivity of $21 \times 10^{-6}$ S (Fig. 14). The in plane conductivity $\sigma$ is defined as $\sigma = (CL)/(hw)$, where $C$ is the lateral conductance of the film, $L$ is the spacing between the two probes, $h$ is the film thickness, and $w$ the probe width. Taking $19.7 - 15.4 = 4.3$ nm for the average film height, the lateral conductivity becomes 0.7 S cm$^{-1}$. Although composite conductivities of up to 150 S cm$^{-1}$ have been reached for relatively thick films using P4VP/$Cu^{2+}$ templated polymerization [24], Ishizu et al. found similar values (compared to this research) for PS-*b*-P4VP/$Cu^{2+}$ templated polymerization in horizontally oriented lamellar samples, however, in their case reaction did not take place in solution as pyrrole vapors were used, and the ions had not been washed from the films after polymerization. Washing led to a considerable decrease in conductivity, which the authors only explained as being caused by the destruction of the microdomain structure, but the effect could also partly originate from the removal of the ions [19]. Furthermore, the value obtained in this research certainly compares positively to the $4 \times 10^{-3}$ S cm$^{-1}$ recently reported by Mou et al. for polypyrrole nano-films prepared by admicellar polymerization [46].

## 4. Conclusion

Single lamellar and cylindrical layers of PS-*b*-P4VP, obtained by washing away PDP from self-assembled thin films of PS-*b*-P4VP(PDP) comb-shaped supramolecules, have been used as templates for chemical oxidation polymerization of pyrrole. On these templates, thin, conducting polypyrrole films of 4–26 nm have been obtained by complexation of $Cu^{2+}$ ions with P4VP and subsequent polymerization in methanol solutions of pyrrole and a small amount of bipyrrole, acting as an initiator. This showed that bipyrrole not only has a favorable influence on solution polymerizations, but also on P4VP/$Cu^{2+}$ templated polymerization. Due to their small thickness, the obtained films are largely transparent, which could be beneficial for the fabrication of polymer-only devices, while single polymer nanorods coated with polypyrrole might serve as conducting nanowires in nanoscale devices.

## References

[1] Bäuerle P. Adv Mater 1993;5:879–86.
[2] Chew SY, Guo ZP, Wang JZ, Chen J, Munroe P, Ng SH, et al. Electrochem Commun 2007;9:941–6.
[3] Dall'Antonia LH, Vidotti ME, Córdoba de Torresi SI, Torresi RM. Electroanal 2002;14:1577–86.
[4] Lewis TW, Spinks GM, Wallace GG, Mazzoldi A, De Rossi D. Synth Met 2001; 122:379–85.
[5] Heeger AJ. Synth Met 2002;125:23–42.
[6] Virji S, Huang J, Kaner RB, Weiller BH. Nano Lett 2004;4:491–6.
[7] Menon VP, Lei J, Martin CR. Chem Mater 1996;8:2382–90.
[8] Kim J, Kwon S, Han S, Min Y. Jpn J Appl Phys 2004;43:5660–4.
[9] Lei J, Cai Z, Martin CR. Synth Met 1992;46:53–69.
[10] Whang YE, Han JH, Motobe T, Watanabe T, Miyata S. Synth Met 1991;45:151–61.
[11] Armes SP. Synth Met 1987;20:365–71.
[12] Machida S, Miyata S, Techagumpuch A. Synth Met 1989;31:311–8.
[13] Mahmud HNME, Kassim A, Zainal Z, Yunus WMM. J Appl Polym Sci 2006;100: 4107–13.
[14] Johnson BJS, Wolf JH, Zalusky AS, Hillmyer MA. Chem Mater 2004;16:2909–17.
[15] Yoon CO, Sung HK, Kim JH, Barsoukov E, Kim JH, Lee H. Synth Met 1999;99: 201–12.
[16] Mohammadi A, Lundström I, Inganäs O. Synth Met 1991;41–43:381–4.
[17] Mohammadi A, Paul DW, Inganäs O, Nilsson JO, Lundström I. J Polym Sci Part A Polym Chem 1994;32:495–502.
[18] Ishizu K, Honda K, Saito R. Polymer 1996;37:3965–70.
[19] Ishizu K, Honda K, Kanbara T, Yamamoto T. Polymer 1994;35:4901–6.
[20] Ishizu K, Tsubaki K, Uchida S. Macromolecules 2002;35:10193–7.
[21] Goren M, Lennox RB. Nano Lett 2001;1:735–8.
[22] Yoo SI, Sohn BH, Zin WC, Jung JC. Langmuir 2004;20:10734–6.
[23] Seo I, Pyo M, Cho G. Langmuir 2002;18:7253–7.
[24] Mohammadi A, Lundström I, Inganäs O, Salaneck WR. Polymer 1990;31:395–9.
[25] van Zoelen W, ten Brinke G. Soft Matter 2009;5:1568–82.
[26] Ruokolainen J, Saariaho M, Ikkala O, ten Brinke G, Thomas EL, Torkkeli M, et al. Macromolecules 1999;32:1152–8.
[27] Ikkala O, ten Brinke G. Science 2002;295:2407–9.
[28] van Zoelen W, Polushkin E, ten Brinke G. Macromolecules 2009;41:8807–14.
[29] Rapoport H, Castagnoli N. J Am Chem Soc 1962;84:2178–81.
[30] Geier GR, Grindrod SC. J Org Chem 2004;69:6404–12.
[31] Li Y, Qian R. Electrochim Acta 2000;45:1727–31.
[32] Rodríguez I, Scharifker BR, Mostany J. J Electroanal Chem 2000;491:117–25.
[33] Thiéblemont JC, Gabelle JL, Planche MF. Synth Met 1994;66:243–7.
[34] Ansari R. Eur J Chem 2006;3:186–201.
[35] Nishikawa H, Tsuchida E. J Phys Chem 1975;79:2072–6.
[36] Tsuchida E, Nishide H, Nishiyama T. J Polym Sci Pol Sym 1974:35–46.

[37] Santana AL, Noda LK, Pires ATN, Bertolino JR. Polym Testing 2004;23:839–45.
[38] Bondzic S. Comb-shaped supramolecules: phase behavior, shear alignment and application. University of Groningen, PhD thesis; 2007.
[39] Yan J, Buckley AM, Greenblatt M. J Non-Cryst Solids 1995;180:180–90.
[40] Moulder JF, Stickle WF, Sobol PE, Bomben KD. Handbook of X-ray photoelectron spectroscopy. Physical Electronics, Inc.; 1995.
[41] Lahaye J, Nanse G, Bagreev A, Strelko V. Carbon 1999;37:585–90.
[42] Tran HD, Shin K, Hong WG, D'Arcy JM, Kojima RW, Weiller BH, et al. Macromol Rapid Comm 2007;28:2289–93.
[43] Dias HVR, Fianchini M, Gamini Rajapakse RM. Polymer 2006;47:7349–54.
[44] Kostić R, Raković D, Stepanyan SA, Davidova IE, Gribov LA. J Chem Phys 1995; 102:3104–9.
[45] Price CC, Nakaoka K. Macromolecules 1971;4:363–9.
[46] Mou CY, Yuan WL, Tsai IS, O'Rear EA, Barraza H. Thin Solid Films 2008;516:8752–6.